

Transformation of nonlinear behaviors: From bright- to dark-gap soliton in a one-dimensional photonic crystal containing a nonlinear indefinite metamaterial defect

Wei Zhang,¹ Yuanyuan Chen,^{1,*} Peng Hou,² Jielong Shi,¹ and Qi Wang¹¹*Department of Physics, Shanghai University, Shanghai 200444, People's Republic of China*²*Shanghai Research Institute of MicroElectronics (SHRIME), Peking University, Shanghai 201203, People's Republic of China*

(Received 15 September 2010; published 10 December 2010)

Nonlinear propagation characteristics are investigated theoretically in a one-dimensional photonic band-gap structure doped with a nonlinear indefinite metamaterial defect for five distinct frequency intervals. It is found from the electric field distribution that there exists the bright gap solitonlike when the nonlinear indefinite metamaterial defect is a cut-off medium, while the dark gap solitonlike can appear in the nonlinear never cut-off defect layer. It is also found that there exists corresponding bistable lateral shift the properties of which are strongly dependent on the permittivity and permeability of nonlinear indefinite metamaterials. Moreover, in contrast to the switch-down threshold value, the switch-up threshold value is more sensitive to the incident frequency.

DOI: [10.1103/PhysRevE.82.066601](https://doi.org/10.1103/PhysRevE.82.066601)

PACS number(s): 41.20.-q, 42.25.Gy, 42.25.Bs, 78.20.Ci

I. INTRODUCTION

It is well known that the artificial structures demonstrated by Shelby *et al.* using a network of thin wires and a periodic arrangement of split ring resonators [1] has received increasing attention over the past few years. Left-handed materials (LHMs) with simultaneously negative permittivity and negative permeability [2], a kind of artificial materials, have several extraordinary electromagnetic characteristics, such as negative refraction [3], reversed Cerenkov effect [2], subdiffraction focusing through perfect lens configuration [4], and so on. Nevertheless, the metamaterials fabricated in experiment are intrinsically anisotropic on account of the orientations of the rings and rods in space [5,6]. Indefinite metamaterial (IMM), one of the anisotropic metamaterials, in which not all the principal components of the electric permittivity and magnetic permeability tensors have the same sign, can offer four different types of dispersion relations [7] and therefore owns much more peculiar electromagnetic properties [8–12]. Recently, with the development of engineered materials, the metamaterial which possesses nonlinear response has been artificially fabricated [13]. Such effects can also be realized in a structure composed of metal wires and split ring resonators embedded in the nonlinear medium [14,15]. Thus, nonlinear indefinite metamaterial can be achieved by means of a reasonable combination of anisotropy with nonlinearity in the IMM, which is expected to produce some interesting physical effects in electromagnetic wave propagation [16–22].

Stimulated by the prospect of potential applications in optical communications [23,24], nonlinear Goos-Hänchen (GH) lateral shift has been extensively studied in different circumstances, including the bistable lateral shift for one-dimensional photonic crystals (1DPCs) doped with nonlinear dielectric [25,26], and the giant bistable lateral shift due to the resonant excitation of surface polaritons in Kretschmann configuration with Kerr nonlinear dielectric [27], as well as

the tunable GH shift in the two-dimensional photonic crystals [28]. In the recent years, gap soliton, another nonlinear optical response of photonic crystals, has also inspired considerable interest, such as zero- n gap soliton in the periodic structure consisting of alternating layers of positive-index and negative-index materials [29,30], bright and dark gap solitons in a negative index Fabry-Pérot *et al.* [31,32], as well as bistability and gap soliton in the defect structure containing single-negative materials [33]. However, most work of nonlinear properties above has been carried out in isotropic materials. In our former paper [26], we have investigated the modulation of bistable lateral shifts in the symmetry structure $(AB)^m N (BA)^m$, where layer A is normal material, layer B is indefinite metamaterial without Kerr-type nonlinearity, and the defect layer N is just a normal Kerr-type nonlinear layer. Now, in spite of the similar structure, indefinite metamaterial B is replaced by normal material, and normal Kerr-type nonlinear layer N is replaced by indefinite metamaterial with Kerr-type nonlinearity. We can obtain some interesting results by studying the nonlinear characteristics and the electric field distribution in the composite structure for five distinct frequency intervals.

The organization of this paper is as follows: in Sec. II, the theoretical model of 1DPC with a nonlinear indefinite metamaterial defect layer will be shown. In Sec. III, we will study the transmission properties and electric field distribution of the defect structure. Finally, the conclusion is given in Sec. IV.

II. THEORETICAL MODEL

We consider a symmetric multilayer stack [34,35] in the background material $C(\epsilon_C, \mu_C)$ as shown in Fig. 1. The stack $(AB)_m A N A (BA)_m$ consists of alternating linear layers of normal materials $A(\epsilon_A, \mu_A)$ and $B(\epsilon_B, \mu_B)$, with a single nonlinear indefinite metamaterial layer N in the middle, where m is

*cyuan@staff.shu.edu.cn

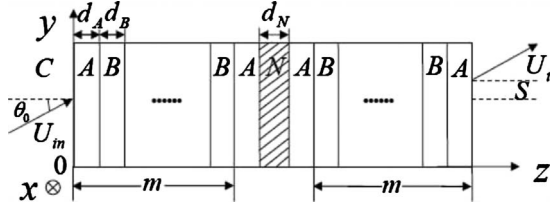


FIG. 1. Schematic of a 1DPC with a nonlinear indefinite metamaterial defect.

the period number. The thicknesses of layers A, B, and N are d_A , d_B , and d_N , respectively.

The anisotropic permittivity and permeability tensors of IMM with Kerr-type nonlinearity are defined as follows [9]:

$$\hat{\epsilon}_N = \begin{pmatrix} \epsilon_{xx} & 0 & 0 \\ 0 & 1 & 0 \\ 0 & 0 & 1 \end{pmatrix}, \quad \hat{\mu}_N = \begin{pmatrix} 1 & 0 & 0 \\ 0 & \mu_{yy} & \mu_{zy} \\ 0 & \mu_{yz} & \mu_{zz} \end{pmatrix}. \quad (1)$$

The diagonal term ϵ_{xx} of $\hat{\epsilon}_N$ is given by $\epsilon_{xx} = \epsilon_x + \chi_3 |E(z)|^2$, where χ_3 and ϵ_x are the Kerr nonlinear coefficient and the diagonal term of the permittivity tensor of IMM without nonlinearity, respectively. Without loss of generality, the diagonal terms ϵ_x , μ_{yy} and μ_{zz} are usually characterized by the frequency-dependent Drude forms [36–38], namely,

$$\epsilon_x = 1 - \frac{1}{\Omega^2}, \quad \mu_{yy} = 1 - \frac{F_y \Omega^2}{\Omega^2 - \Omega_{ry}^2}, \quad \mu_{zz} = 1 - \frac{F_z \Omega^2}{\Omega^2 - \Omega_{rz}^2}, \quad (2)$$

where $\Omega = \omega / \omega_p$ is the normalized frequency, $\Omega_{ry} = \omega_{ry} / \omega_p$ and $\Omega_{rz} = \omega_{rz} / \omega_p$ are the normalized magnetic resonant frequencies, ω_p is the electric plasma frequency, and F_y and F_z are the constants between zero and unity. These physical parameters are all structure dependent [39–42]. Note that the off-diagonal terms μ_{zy} and μ_{yz} would not alter the results in our paper.

In our analysis, consider a wave beam of angular frequency ω incident from the background upon this 1DPC at an angle θ_0 . In the absence of losses, we assume that the wave vector locates at the y - z plane and the incident electric field is $\vec{E} = \hat{x} E_0 \exp[i(\beta y + k_{Cz} z - \omega t)]$, where β and k_{Cz} are y and z components of the incident wave vector, where $\beta = k_C \sin \theta_0 = k_0 \sqrt{\epsilon_C \mu_C} \sin \theta_0$, $k_0 = \omega / c$, and $k_{Cz} = k_C \cos \theta_0$. Here we only concentrate on the TE mode (s -polarized light) and the treatment for the TM mode (p -polarized light) is similar.

Generally, the electric and magnetic fields at two sides of some layer can be related via transfer matrix [43]. For the indefinite metamaterial layer N with Kerr-type nonlinearity, the transfer matrix should be modified in the form [44,45]

$$M_N = \frac{k_0}{k_{z+} + k_{z-}} \begin{pmatrix} \frac{k_{z-}}{k_0} \exp(-ik_{z+} d_N) + \frac{k_{z+}}{k_0} \exp(ik_{z-} d_N) & \mu_{yy} [\exp(-ik_{z+} d_N) - \exp(ik_{z-} d_N)] \\ \frac{k_{z-} k_{z+}}{k_0^2 \mu_{yy}} [\exp(-ik_{z+} d_N) - \exp(ik_{z-} d_N)] & \frac{k_{z+}}{k_0} \exp(-ik_{z+} d_N) + \frac{k_{z-}}{k_0} \exp(ik_{z-} d_N) \end{pmatrix}, \quad (3)$$

where k_{z+} and k_{z-} are the z components of wave vector for the forward and backward propagating waves, which are given by

$$k_{z\pm} = k_{Nz} (1 + U_{\pm} + 2U_{\mp})^{1/2}, \quad (4)$$

with $U_{\pm} = \chi_3 k_0^2 |A_{\pm}|^2 / k_{Nz}^2$. Here A_+ and A_- are the amplitudes of the forward and backward waves and k_{Nz} is the z component of wave vector for IMM without nonlinearity, which is shown as

$$k_{Nz}^2 = \frac{\mu_{yy}}{\mu_{zz}} \left(\frac{\omega^2}{c^2} \epsilon_x \mu_{zz} - \beta^2 \right). \quad (5)$$

It is noted that the choice of the sign of the wave vector k_{Nz} must ensure the Poynting vector inside the indefinite medium to point away from the interface separating the incident and indefinite medium. Thus, according to Refs. [46,47], k_{Nz} and μ_{yy} must keep the same sign.

By using fixed point iteration [48], we solve a set of coupled nonlinear equations with respect U_{\pm} and obtain the

explicit form of M_N . Then the transmission coefficient can be expressed by

$$t = \frac{2p}{[M_{11} + M_{12}p]p + [M_{21} + M_{22}p]}, \quad (6)$$

where $p = \sqrt{\epsilon_C \mu_C} \cos \theta_0$ and M_{ij} are the elements of 2×2 matrix M for the composite medium. The power transmittance T is identified as $T = t \cdot t^* = U_t / U_{in}$, where U_{in} and U_t are the incident and transmitted intensity, respectively. According to the stationary phase method [49], the lateral shift of the beam through the composite structure is obtained as follows:

$$s = - \left. \frac{d\phi_t}{d\beta} \right|_{\theta=\theta_0} = - \frac{1}{\sqrt{\epsilon_C \mu_C} k_0 \cos \theta_0} \left. \frac{d\phi_t}{d\theta} \right|_{\theta=\theta_0}, \quad (7)$$

where ϕ_t is the phase shift of transmitted beam and $\phi_t = \arctan[\text{Im}(t) / \text{Re}(t)]$.

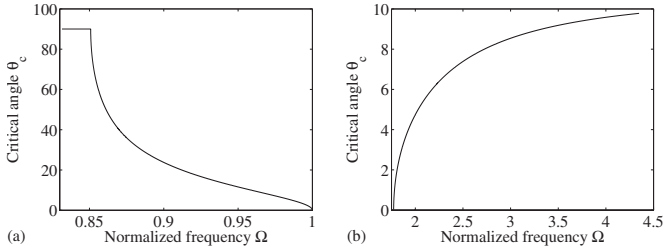


FIG. 2. The relationship between the critical angle θ_c (deg) and the normalized frequency Ω . (a) $0.8315 < \Omega < 1$; (b) $1.7728 < \Omega$.

III. COMPUTATION RESULTS AND DISCUSSION

Since the components of the anisotropic permittivity and permeability tensors in the IMM without nonlinearity can be either positive or negative by changing corresponding structure parameters and incident frequencies according to Eq. (2), the dispersion relation of such medium, given by Eq. (6), can be elliptic or hyperbolic depending on the signs of the parameters ε_x , μ_{yy} , and μ_{zz} . Therefore different types of nonlinear indefinite metamaterials will lead to different properties of one-dimensional nonlinear photonic crystals. To numerically analyze the features of electromagnetic wave propagating 1DPC under consideration, the parameters are taken in our calculation as follows: $F_y=0.56$, $F_z=0.78$, $\omega_p/2\pi=18.4$ GHz, $\omega_{ry}/2\pi=\omega_{rz}/2\pi=15.3$ GHz, $\chi_3=0.01$ [25,50–53] for nonlinear indefinite metamaterial N , $\varepsilon_A=5.29$, $\varepsilon_B=1.71$, $\varepsilon_C=6.25$, $\mu_A=\mu_B=\mu_C=1.00$ [45] for normal materials A , B , and C , and $m=3$. The parameters ε_x , μ_{yy} , and μ_{zz} of nonlinear indefinite metamaterial are all frequency dependent, and thus they have different signs in different frequency ranges. For clarity, we consider five distinct frequency intervals, specified in the following, respectively.

(i) $0 < \Omega < 0.8315$, where $\varepsilon_x < 0$, $\mu_{yy} > 0$, and $\mu_{zz} > 0$. The dispersion relation of such type which is called always cut-off medium is that k_{Nz}^2 is always negative, and the transverse wave vector k_{Nz} is always imaginary. Because of this, any propagating or evanescent waves cannot propagate into the always cut-off medium and all incident beams are totally reflected, i.e., the IMM here behaves like an electric or magnetic plasma. Hence there will be no transmitted beam shift at any condition.

(ii) $0.8315 < \Omega < 1$, in which $\varepsilon_x < 0$, $\mu_{yy} < 0$ and $\mu_{zz} < 0$. In such a case, when $\varepsilon_x \mu_{yy} > \varepsilon_C \mu_C$ from Eq. (6), the transmitted beam shift always exists no matter how the incident angle changes; however, when $\varepsilon_x \mu_{yy} < \varepsilon_C \mu_C$, there exists a critical angle $\theta_c = \arcsin \sqrt{\varepsilon_x \mu_{yy} / \varepsilon_C \mu_C}$ which is shown in Fig. 2(a). If the incident angle $\theta_0 < \theta_c$, the transverse wave vector k_{Nz} becomes real and the electromagnetic wave can propagate in the composite structure containing such material which is named as cut-off medium. Note that the incident angle θ_0 should also be selected smaller than the critical angle of total reflection in the surface between the background material C and normal material A . In this case, the IMM without nonlinearity has negative refraction properties.

(iii) $1 < \Omega < 1.2536$, where $\varepsilon_x > 0$, $\mu_{yy} < 0$, and $\mu_{zz} < 0$. This is another case of always cut-off medium and the behavior of propagation is similar with (i).

(iv) $1.2536 < \Omega < 1.7728$, where $\varepsilon_x > 0$, $\mu_{yy} > 0$, and $\mu_{zz} < 0$. It can be found from Eq. (6) that the transverse wave

vector k_{Nz} is always real. Any incident waves impinging the 1DPC containing this never cut-off medium with Kerr-type nonlinearity will be changed into propagating waves no matter whether the incident waves are propagating or evanescent. Therefore the lateral shift of the transmitted wave always exists for all incident angles.

(v) $1.7728 < \Omega$, in which $\varepsilon_x > 0$, $\mu_{yy} > 0$, and $\mu_{zz} > 0$. For this material, another case of cut-off medium, if the incident angle satisfies the same condition $\theta_0 < \theta_c = \arcsin \sqrt{\varepsilon_x \mu_{yy} / \varepsilon_C \mu_C}$ shown in Fig. 2(b), we can also get the transmitted beam shift. In this interval, the IMM can be regarded as a conventional anisotropic material.

Below, we will focus on cases (ii), (iv), and (v) to discuss the nonlinear propagation properties in detail.

A. Case A: $0.8315 < \Omega < 1$ ($\varepsilon_x < 0$, $\mu_{yy} < 0$, and $\mu_{zz} < 0$)

It is known that when a defect without nonlinearity is introduced in the photonic band-gap structures, the corresponding linear defect mode will appear in the forbidden band [54]. An incident wave which is tuned at the linear defect mode frequency can pass through this structure with almost no reflection. But the incident light frequency is tuned in the forbidden band (not at the linear defect mode frequency), the electric field will decrease exponentially in the structure. In the following calculations, we take $\theta_0=23^\circ$, $\omega/2\pi=16.123$ GHz, $d_A=\frac{\lambda_p}{4\sqrt{\varepsilon_A\mu_A}}$, $d_B=\frac{\lambda_p}{4\sqrt{\varepsilon_B\mu_B}}$, and $d_N=\frac{\lambda_p}{2}$, where $\lambda_p=\frac{2\pi c}{\omega_p}$ is plasma wavelength. It is noted that the above physical parameters should be correctly chosen in order to obtain defect mode and corresponding bistable lateral shift at the same time. Here negative ε_x and positive χ_3 correspond to defocusing effects in the beam propagation. We tune the incident light frequency ω near but bigger than the linear defect mode Ω_0 ($\Omega_0/2\pi=16.01$ GHz) without nonlinearity, and when the incident light intensity increases, the magnitude of ε_{xx} decreases with the local light intensity in such a defect layer, and hence the corresponding defect mode frequency increases toward the incident wave frequency ω [55]. This means that the composite structure containing this type of nonlinear indefinite metamaterial can produce a negative feedback on the incident light [56]. Therefore, optical bistability will occur when the defect mode frequency almost equals to the incident light frequency ω . Figure 3(a) shows a typical S-shape bistability curve, where points 1 and 2 represent the switch-down and switch-up threshold values, respectively. The threshold of optical bistability is dependent on how far away the incident wave frequency ω deviates from the linear defect mode Ω_0 [56]. Now, we investigate variation in the switch-down I_1 and switch-up I_2 threshold values with ω . It can be seen from Fig. 3(b) that as ω moves far from Ω_0 , the switch-down threshold value I_1 increases slightly, but the switch-up threshold value I_2 increases evidently. However, when ω comes very close to or even exceeds Ω_0 , the bistable behavior will disappear.

And we also plot the variation in the corresponding lateral shift S with the incident intensity I_{in} in Fig. 4(a). It can be shown that when the incident intensity I_{in} is smaller than point 2, the lateral shift is positive originally. But the lateral shift suddenly jumps to a negative value when I_{in} arrives to

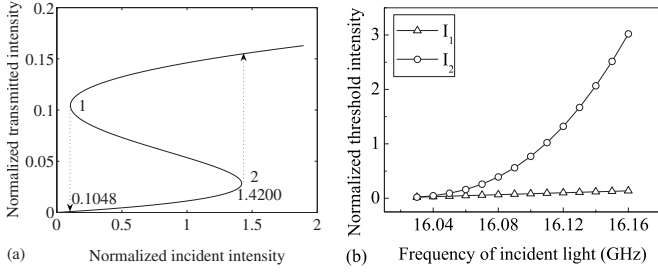


FIG. 3. (a) The variation in the normalized transmitted intensity with the normalized incident intensity. (b) The variation in the normalized threshold values with the incident light frequency ω , where the corresponding linear defect mode frequency $\Omega_0/2\pi = 16.01$ GHz. The incident and transmitted intensities are normalized by $\chi_3 k_0^2/k_{Nz}^2$.

point 2. On the other hand, with the decreasing in I_{in} from a higher value, the negative lateral shift increases in the beginning. However, the lateral shift drops to a positive value suddenly when I_{in} decreases to point 1. To understand it more clearly, we have investigated ϕ_t as a function of β with various I_{in} as shown in Fig. 4(b). It can be found that when the incident intensity increases between 1.368 00 and 1.534 00 near point 2, there is an abrupt change in the phase shift ϕ_t . This means that the lateral shift changes quickly with the incident intensity increasing up to point 2. On the contrary, when the incident intensity decreases between 0.152 60 and 0.085 09 near point 1, there also exists an abrupt change in ϕ_t which cause the lateral shift to jump to a smaller value. Note that the positive slope of ϕ_t leads to the negative lateral shift and that the phase shift ϕ_t is plotted between $-\pi/2$ and $\pi/2$ which can produce a sudden change at some fixed β . In one word, the hysteretic behavior of S with the variation in I_{in} is closely related to the phase shift, which is explained by the reshaping effect, that is, the constructive and destructive interference between each plane wave components, due to the different phase shifts of each transmitted plane wave components transmitted the IDPC structure.

In addition, we have also investigated the electric field distribution in the system corresponding to the high-transmission state [point 1 in Fig. 3(a)]. It is found from Fig. 5(a) that the bright gap solitonlike can be formed in the

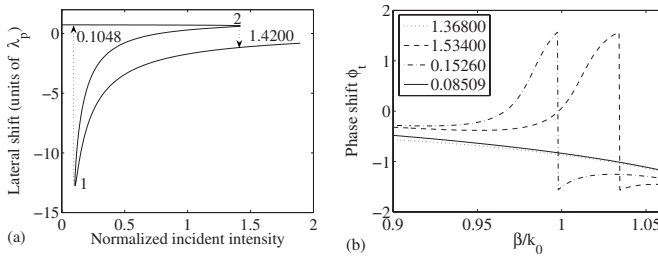


FIG. 4. (a) The variation in the lateral shift on the normalized incident intensity, where the physical parameters are all the same with Fig. 3(a). (b) The phase shift ϕ_t as a function of β for different I_{in} . β is rescaled by β/k_0 . The normalized incident intensities 1.368 00 and 1.534 00 (0.152 60 and 0.085 09) are near the point 2 (1).

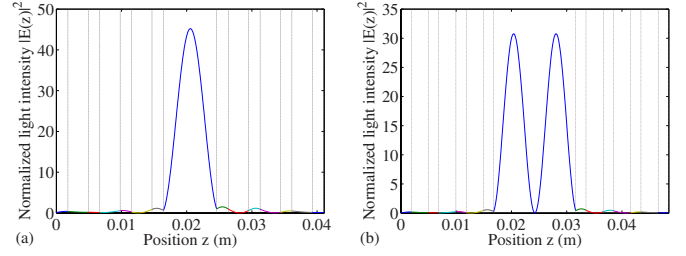


FIG. 5. (Color online) (a) The electric field distribution in the defect structure containing nonlinear cut-off metamaterial corresponding to the high-transmission state (point 1). (b) The double bright gap solitonlike distribution in the nonlinear cut-off metamaterial defect layer, where $d_A = 1.05 \frac{\lambda_p}{4\sqrt{\epsilon_A \mu_A}}$, $d_N = 1.82 \frac{\lambda_p}{2}$, and the corresponding incident light frequency is $\omega/2\pi = 15.966$ GHz. Other physical parameters are all the same with Fig. 3(a).

nonlinear indefinite metamaterial defect layer N and the electric field reaches the peak at the center of the defect layer. It is noted that to realize the bright gap solitonlike, one should apply a larger pump field intensity than the switch-up threshold value I_2 , then decrease it to the intensity corresponding to the switch-down threshold value I_1 . With the increasing of the thicknesses d_N of layer N , the electric field is periodic with the distance in the defect layer by changing some corresponding physical parameters. From Fig. 5(b), we can observe that there exists a double bright gap solitonlike distribution owing to the occurrence of optical oscillation in the nonlinear indefinite metamaterial defect layer N .

B. Case B: $1.2536 < \Omega < 1.7728$ ($\epsilon_x > 0$, $\mu_{yy} > 0$, and $\mu_{zz} < 0$)

As we all know, both positive ϵ_x and χ_3 characterizes self-focusing effects in the beam propagation. Here, we choose the incident light frequency ω near but smaller than the linear defect mode Ω_0 without nonlinearity, and the magnitude of ϵ_{xx} increases in the defect layer as the incident light intensity increases, and therefore the corresponding defect mode frequency decreases toward ω . In this case, the doped structure can produce a positive feedback on the incident light which is opposite to above case. Thus, optical bistability will appear in the optical system with a positive feedback. Next, tuning the incident light frequency, we study the variation in threshold values with the incident light frequency. It can also be observed from Fig. 6 that the switch-up threshold value I_2 increases rapidly when ω is tuned away from Ω_0 , while the switch-down threshold value I_1 remains almost unchanged.

Figure 7(a) shows that the bistable lateral shift can be switched from positive to negative at the switch-up threshold I_2 and from negative to positive at the switch-down threshold I_1 , which exists in above case. But the negative peak can reach a much great value. Meanwhile, we have also investigated the phase shift ϕ_t for different I_{in} as shown in Fig. 7(b). We can observe that around some fixed β (e.g., $\beta/k_0 = 1.0763$) the phase shift ϕ_t also experiences abrupt changes near the switch-up and switch-down thresholds, which results in the bistable lateral shift.

In Fig. 8(a), we see that the normalized light intensity $|E(z)|^2$ near the defect layer reaches about 18 much larger

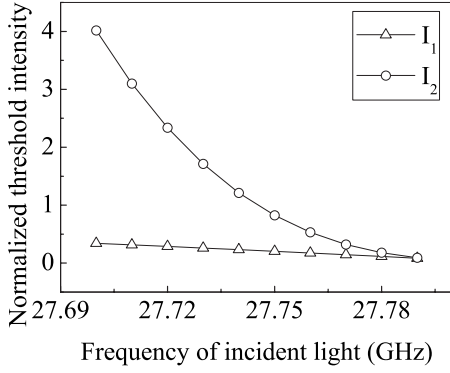


FIG. 6. The variation in the normalized threshold values with the incident light frequency ω , where $\theta_0=25.5^\circ$, $d_A=1.2\frac{\lambda_p}{4\sqrt{\epsilon_A\mu_A}}$, $d_B=1.1\frac{\lambda_p}{4\sqrt{\epsilon_B\mu_B}}$, $d_N=0.5\frac{\lambda_p}{2}$, and $\Omega_0/2\pi=27.82$ GHz.

than the incident intensity, but the field intensity in the defect layer is smaller than that in the surrounding layers. Then the electric field corresponding to the high-transmission state forms a dark gap solitonlike in the nonlinear never cut-off medium layer N with the bottom locating at the center of layer N . In Ref. [7], never cut-off medium can exhibit some anomalous dispersion relation not readily observed in the ordinary material. When a wave beam propagates through a 1DPC containing this type of nonlinear indefinite metamaterial, multiple transmissions occur due to multiple reflections between layers. The whole field intensity distribution in the structure is the coherent superposition between reflected fields from boundaries of different layers. Owing to the special relations of ϵ_x , μ_{yy} , and μ_{zz} with the incident light frequency ω , the variation in incident intensity changes the equivalent refractive index of the nonlinearity, which affects each reflected fields. Thus, this causes the anomalous electric field distribution in the structure shown in Fig. 8(a). We can also observe from Fig. 8(b) that there exists a double dark gap solitonlike distribution in the nonlinear indefinite metamaterial defect layer N with the increasing of the thicknesses d_N .

C. Case C: $1.7728 < \Omega$ ($\epsilon_x > 0$, $\mu_{yy} > 0$, and $\mu_{zz} > 0$)

Optical bistability is obtained in the doped structure containing such type of nonlinear indefinite metamaterial which

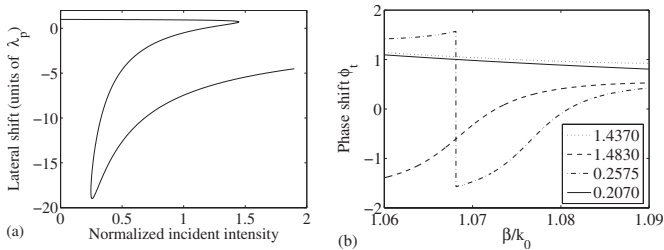


FIG. 7. (a) The variation in the lateral shift on the normalized incident intensity with $\omega/2\pi=27.735$ GHz. (b) The phase shift ϕ_t as a function of β for different I_{in} , where the corresponding switch-up and switch-down thresholds are 1.448 and 0.2465, respectively.

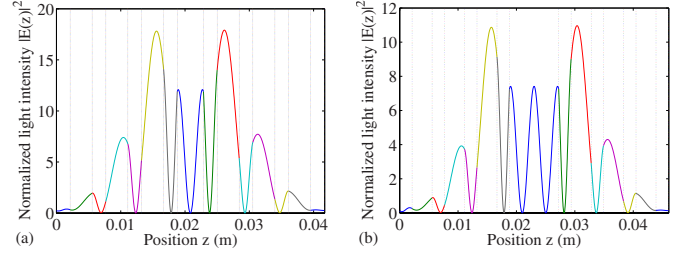


FIG. 8. (Color online) (a) The electric field distribution in the defect structure containing nonlinear never cut-off metamaterial corresponding to the high-transmission state. (b) The double dark gap solitonlike distribution in the nonlinear never cut-off metamaterial defect layer, where $d_N=1.035\frac{\lambda_p}{2}$, and the corresponding incident light frequency is $\omega/2\pi=27.485$ GHz.

can also produce a positive feedback. Figure 9 gives the variation in the threshold values I_1 and I_2 with the incident light frequency ω .

There exists positive bistable lateral shift shown in Fig. 10(a) in this condition and the phase shift ϕ_t in Fig. 10(b) can account for the hysteretic behavior of S . Figure 11(a) gives the electric field distribution corresponding to the high-transmission state in 1DPC containing such metamaterial, another case of nonlinear cut-off metamaterial. The bright gap solitonlike can also be found in the defect layer N which exists in case A. Meanwhile, the double bright gap solitonlike distribution shown in Fig. 11(b) can be realized in the nonlinear cut-off metamaterial defect layer N with the increasing of d_N .

IV. CONCLUSION

In summary, we have investigated the nonlinear responses in a 1DPC with a nonlinear indefinite metamaterial defect layer centered in the structure for five distinct frequency intervals. The electric field distribution in the defect structure is studied in detail. It is found that the bright gap solitonlike is found when the nonlinear indefinite metamaterial defect is a cut-off medium, while the dark gap solitonlike is found in the nonlinear never cut-off defect layer. This is the most important and most interesting discovery which is distinct

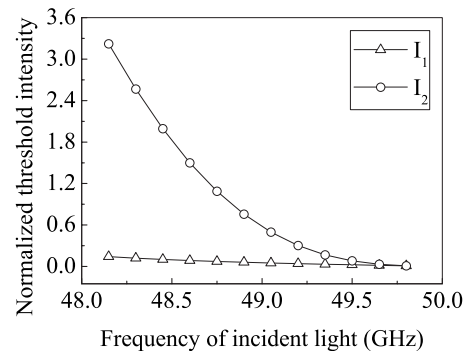


FIG. 9. The variation in the normalized threshold values with the incident light frequency ω , where $\theta_0=5.5^\circ$, $d_A=1.19\frac{\lambda_p}{4\sqrt{\epsilon_A\mu_A}}$, $d_B=1.09\frac{\lambda_p}{4\sqrt{\epsilon_B\mu_B}}$, $d_N=0.78\frac{\lambda_p}{2}$, and $\Omega_0/2\pi=50.02$ GHz.

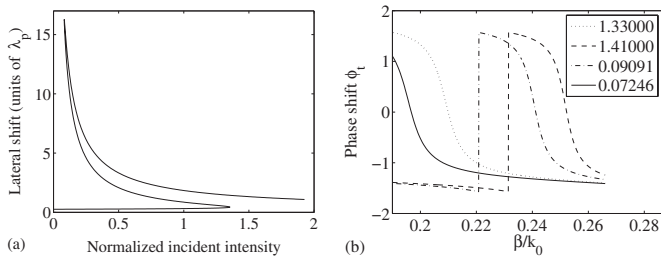


FIG. 10. (a) The variation in the lateral shift on the normalized incident intensity with $\omega/2\pi=48.65$ GHz. (b) The phase shift ϕ_t as a function of β for different I_{in} , where the corresponding switch-up and switch-down thresholds are 1.354 and 0.082 41, respectively.

from the results obtained and reported in Ref. [26]. The transformation between the bright and dark solitons cannot be realized in the normal Kerr-type nonlinear layer in our former paper [26]. In the current paper, there also exists the hysteresis response between the incident light intensity and the lateral shift of the transmitted beam which can be explained by the phase shift for different incident intensities. In addition, the variation in the switch-up and switch-down threshold values with the frequency offset between the incident light frequency and the linear defect mode is further discussed in this paper. All these phenomena will lead to potential applications in integrated optics and optical switches.

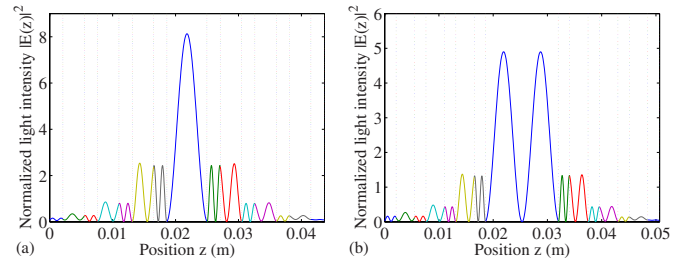


FIG. 11. (Color online) (a) The electric field distribution in the defect structure containing nonlinear cut-off metamaterial corresponding to the high-transmission state. (b) The double bright gap solitonlike distribution in the nonlinear cut-off metamaterial defect layer, where $d_N=1.638\frac{\lambda_p}{2}$, and the corresponding incident light frequency is $\omega/2\pi=48.96$ GHz.

ACKNOWLEDGMENTS

This work was supported in part by the National Natural Science Foundation of China (Grants No. 60677030, No. 60808002, and No. 108040707), the Science and Technology Commission of Shanghai Municipality, China (Grant No. 08JC14097), the Shanghai Leading Academic Discipline Program, China (Grant No. S30105), and the Foundation Project of Science and Technology Commission of Shanghai (Grant No. 10R21421000).

-
- [1] R. A. Shelby, D. R. Smith, and S. Schultz, *Science* **292**, 77 (2001).
- [2] V. G. Veselago, *Sov. Phys. Usp.* **10**, 509 (1968).
- [3] D. R. Smith and N. Kroll, *Phys. Rev. Lett.* **85**, 2933 (2000).
- [4] J. B. Pendry, *Phys. Rev. Lett.* **85**, 3966 (2000).
- [5] R. Marqués, F. Mesa, J. Martel, and F. Medina, *IEEE Trans. Antennas Propag.* **51**, 2572 (2003).
- [6] R. Marqués, F. Medina, and R. Rafii-El-Idrissi, *Phys. Rev. B* **65**, 144440 (2002).
- [7] D. R. Smith and D. Schurig, *Phys. Rev. Lett.* **90**, 077405 (2003).
- [8] D. Schurig and D. R. Smith, *Appl. Phys. Lett.* **82**, 2215 (2003).
- [9] D. R. Smith, P. Kolinko, and D. Schurig, *J. Opt. Soc. Am. B* **21**, 1032 (2004).
- [10] D. R. Smith, D. Schurig, J. J. Mock, P. Kolinko, and P. Rye, *Appl. Phys. Lett.* **84**, 2244 (2004).
- [11] L. B. Hu and S. T. Chui, *Phys. Rev. B* **66**, 085108 (2002).
- [12] T. M. Grzegorzcyk, Z. M. Thomas, and J. A. Kong, *Appl. Phys. Lett.* **86**, 251909 (2005).
- [13] M. Lapine, M. Gorkunov, and K. H. Ringhofer, *Phys. Rev. E* **67**, 065601(R) (2003).
- [14] A. A. Zharov, I. V. Shadrivov, and Y. S. Kivshar, *Phys. Rev. Lett.* **91**, 037401 (2003).
- [15] V. M. Agranovich, Y. R. Shen, R. H. Baughman, and A. A. Zakhidov, *Phys. Rev. B* **69**, 165112 (2004).
- [16] W. Dickson, G. A. Wurtz, P. Evans, D. O'Connor, R. Atkinson, R. Pollard, and A. V. Zayats, *Phys. Rev. B* **76**, 115411 (2007).
- [17] F. W. Ye, B. A. Malomed, Y. J. He, and B. Hu, *Phys. Rev. A* **81**, 043816 (2010).
- [18] C. W. Qiu, A. Novitsky, H. Ma, and S. B. Qu, *Phys. Rev. E* **80**, 016604 (2009).
- [19] A. Komarov, K. Komarov, D. Meshcheriakov, F. Amrani, and F. Sanchez, *Phys. Rev. A* **82**, 013813 (2010).
- [20] I. V. Shadrivov, A. A. Sukhorukov, Y. S. Kivshar, A. A. Zharov, A. D. Boardman, and P. Egan, *Phys. Rev. E* **69**, 016617 (2004).
- [21] A. Kul'minskii, *Phys. Rev. A* **62**, 023806 (2000).
- [22] G. D. Xu, T. Pan, T. C. Zang, and J. Sun, *J. Phys. D* **42**, 045303 (2009).
- [23] T. Sakata, M. Makihara, H. Togo, F. Shimokawa, and K. Kaneko, *Proc. SPIE* **4534**, 55 (2001).
- [24] T. Sakata, H. Togo, and F. Shimokawa, *Appl. Phys. Lett.* **76**, 2841 (2000).
- [25] P. Hou, Y. Y. Chen, X. Chen, J. L. Shi, and Q. Wang, *Phys. Rev. A* **75**, 045802 (2007).
- [26] W. Zhang, Y. Y. Chen, J. L. Shi, and Q. Wang, *Phys. Rev. E* **81**, 046603 (2010).
- [27] H. C. Zhou, X. Chen, P. Hou, and C. F. Li, *Opt. Lett.* **33**, 1249 (2008).
- [28] A. Matthews and Y. Kivshar, *Phys. Lett. A* **372**, 3098 (2008).
- [29] R. S. Hegde and H. G. Winful, *Microwave Opt. Technol. Lett.* **46**, 528 (2005).
- [30] R. S. Hegde and H. G. Winful, *Opt. Lett.* **30**, 1852 (2005).
- [31] G. D'Aguzzo, N. Mattiucci, M. Scalora, and M. J. Bloemer, *Phys. Rev. Lett.* **93**, 213902 (2004).

- [32] G. D'Aguanno, N. Mattiucci, M. Scalora, and M. J. Bloemer, *Laser Phys.* **15**, 590 (2005).
- [33] S. M. Wang, C. J. Tang, T. Pan, and L. Gao, *Phys. Lett. A* **348**, 424 (2006).
- [34] S. D. Gupta, *J. Opt. Soc. Am. B* **6**, 1927 (1989).
- [35] L. G. Wang and S. Y. Zhu, *Opt. Lett.* **31**, 101 (2006).
- [36] D. R. Smith, W. J. Padilla, D. C. Vier, S. C. Nemat-Nasser, and S. Schultz, *Phys. Rev. Lett.* **84**, 4184 (2000).
- [37] Th. Koschny, P. Markoš, E. N. Economou, D. R. Smith, D. C. Vier, and C. M. Soukoulis, *Phys. Rev. B* **71**, 245105 (2005).
- [38] R. W. Ziolkowski and E. Heyman, *Phys. Rev. E* **64**, 056625 (2001).
- [39] L. Zhou, C. T. Chan, and P. Sheng, *Phys. Rev. B* **68**, 115424 (2003).
- [40] D. Schurig, J. J. Mock, and D. R. Smith, *Appl. Phys. Lett.* **88**, 041109 (2006).
- [41] R. P. Liu, Q. Cheng, T. Hand, J. J. Mock, T. J. Cui, S. A. Cummer, and D. R. Smith, *Phys. Rev. Lett.* **100**, 023903 (2008).
- [42] D. R. Smith, J. J. Mock, A. F. Starr, and D. Schurig, *Phys. Rev. E* **71**, 036609 (2005).
- [43] N. H. Liu, S. Y. Zhu, H. Chen, and X. Wu, *Phys. Rev. E* **65**, 046607 (2002).
- [44] G. S. Agarwal and S. D. Gupta, *Opt. Lett.* **12**, 829 (1987).
- [45] S. D. Gupta and G. S. Agarwal, *J. Opt. Soc. Am. B* **4**, 691 (1987).
- [46] X. Chen and C. F. Li, *Phys. Rev. E* **69**, 066617 (2004).
- [47] H. X. Da, C. Xu, Z. Y. Li, and Galina Kraftmakher, *Phys. Rev. E* **71**, 066612 (2005).
- [48] S. Dutta Gupta and D. S. Ray, *Phys. Rev. B* **38**, 3628 (1988).
- [49] T. E. Hartman, *J. Appl. Phys.* **33**, 3427 (1962).
- [50] M. W. Feise, I. V. Shadrivov, and Y. S. Kivshar, *Phys. Rev. E* **71**, 037602 (2005).
- [51] R. Ruppin, *Phys. Lett. A* **277**, 61 (2000).
- [52] C. J. Fu, Z. M. Zhang, and D. B. Tanner, *J. Heat Transfer* **127**, 1046 (2005).
- [53] S. M. Vuković, N. B. Aleksić, and D. V. Timotijević, *Eur. Phys. J. D* **39**, 295 (2006).
- [54] E. Yablonovitch, T. J. Gmitter, R. D. Meade, A. M. Rappe, K. D. Brommer, and J. D. Joannopoulos, *Phys. Rev. Lett.* **67**, 3380 (1991).
- [55] R. Wang, J. Dong, and D. Y. Xing, *Phys. Status Solidi* **200**, 529 (1997).
- [56] R. Wang, J. Dong, and D. Y. Xing, *Phys. Rev. E* **55**, 6301 (1997).